

**SUB-DOPPLER TWO-PHOTON SPECTRUM OF ASYMMETRIC ROTOR MOLECULES:
ANALYSIS OF THE ^{99}Q ROTATIONAL BRANCH
OF THE $\text{S}_1(^1\text{B}_{2u})14^1 \leftarrow \text{S}_0(^1\text{A}_{1g})$ SYSTEM OF BENZENE- d_1**

Alfredo E. BRUNO¹, Eberhard RIEDLE and Hans J. NEUSSER

*Institut für Physikalische und Theoretische Chemie, Technische Universität München,
Lichtenbergstrasse 4, D-8046 Garching, West Germany*

Received 16 December 1985; in final form 12 March 1986

The Doppler-free two-photon excitation spectrum of the ^{99}Q branch of the 14_0^1 vibrational band of the $\text{S}_1(^1\text{B}_{2u}) \leftarrow \text{S}_0(^1\text{A}_{1g})$ transition of benzene- d_1 has been recorded using a cw single-mode dye laser coupled to an external concentric resonator. The spectrum has been analysed using a non-rigid Watson Hamiltonian. More than 200 lines with J up to 20 have been assigned and the rotational constants which best reproduce the spectrum are $A'_v = 0.181435$, $B'_v = 0.169990$, $C'_v = 0.089055 \text{ cm}^{-1}$. The $K_a = \text{odd}$ lines of the $^{99}\text{Q}_5(J)$ subbranch show small and quite regular perturbations of $60 \pm 5 \text{ MHz}$ which are probably due to a coupling to another vibrational state of the S_1 manifold.

1. Introduction

It is now well established that two-photon absorption provides new spectral information preferentially in molecules of high symmetry; this has been demonstrated for a series of molecules [1]. The transition studied in most detail by two-photon absorption techniques is the $\text{S}_1(^1\text{B}_{2u}) \leftarrow \text{S}_0(^1\text{A}_{1g})$ system of benzene [1–3]. After the detection of hitherto unknown vibrational frequencies [4], sub-Doppler resolution, using two-photon absorption, has been achieved at this laboratory in several spectroscopic and photophysical studies [5–7]. Recently we identified perturbations [8,9] leading to line splittings as large as 1 GHz in the ^{99}Q branch of the 14_0^1 vibronic band of this molecule. Although some hypotheses about the nature of the perturbing vibrational state have been made [8], the presently available information precludes the unequivocal identification of it. In order to gain more insight into the problem we are presently studying several isotopic species of benzene whose spectra have previously been explored by two-photon absorption techniques at vibrational resolution [2,3,

10]. It is of interest to know how the alternation of vibrational frequencies and the change of molecular point groups influence the coupling mechanism. In this publication we report the first results of these spectroscopic studies on benzene- d_1 .

The symmetry- and parity-forbidden two-photon $\text{S}_1 \leftarrow \text{S}_0$ electronic transition of benzene is induced by vibrational modes of b_{2u} symmetry and, to a lesser extent, by e_{1u} and e_{2u} symmetries [1,2]. Upon monodeuteration the D_{6h} symmetry of benzene reduces* to C_{2v} and the vibrational selection rules become less stringent, but nevertheless most of the features of the vibrational structure of the S_1 spectrum remain common to both species [2,3,10]. The $14_0^1(b_{2u})$ band (b_1 in C_{2v}) studied here is, for instance, very strong in the two-photon spectra of both benzene- h_6 [2] and benzene- d_1 .

Much greater changes than those observed in the vibrational spectrum occur in the rotational structure of the vibronic band systems of both isotopic species. This is primarily because benzene- d_1 is a fairly asym-

* Although it is not formally correct from a symmetry point of view, we use here the same labelling of the vibronic species in benzene- d_1 as in benzene- h_6 .

¹ 1985 Alexander von Humboldt fellow.

metric molecule with an asymmetry parameter $\kappa = 0.7515$ in its ground electronic state [11] while benzene- \hbar_6 is an oblate symmetric top. As we show in this work, about 200 transitions appear in the first wavenumber of the ${}^{\text{q}}\text{qQ}$ branch (blue edge) of the benzene- d_1 spectrum while in benzene- \hbar_6 there are only about 60 transitions in the same portion of the equivalent spectrum.

Even though the rotational analysis of the asymmetric rotor benzene- d_1 is complicated at first sight, there is the advantage that microwave spectra of the S_0 ground electronic state are available (these are not available for benzene- \hbar_6). Oldani and Bauder [11] have evaluated the ground-state rotational constants including quartic centrifugal constants from a fit to 20 lines of the FT microwave spectrum. These constants have been used in the present analysis.

In this work, a point of particular emphasis is the determination of quartic centrifugal distortion constants. The present analysis of the room-temperature Doppler-free $S_1(1^1\text{B}_{2u})14^1 \leftarrow S_0(1^1\text{A}_{1g})$ spectrum of $\text{C}_6\text{H}_5\text{D}$ provides the first determination of some of the centrifugal distortion constants of the excited electronic state of a large molecule from a line-resolved spectrum. The resolution of the many lines has been possible due to the elimination of room-temperature Doppler broadening by two-photon absorption. The resulting spectrum displays lines with high and low rotational quantum numbers at the same time.

2. Experimental

The apparatus used in this work has been described in detail in a previous publication [7]. A cw Kr^+ -laser-pumped single-mode ring dye laser system (coumarin 102) provided an output beam with a frequency width of 1 MHz and a power of some 150 mW around 504 nm. The dye laser light is coupled to an external concentric cavity to enhance the excitation probability while retaining the original linewidth. The observed fluorescence signal originating from the Doppler-free absorption of two counterpropagating photons of identical polarization inside the external resonator is more than 50 times stronger than otherwise obtained. The signal-to-noise improvement allows pressure reductions inside the fluorescence cell

to about 500 mTorr and hence collision broadening effects are minimized. The dye-laser frequency scans were monitored by a temperature-stabilized confocal interferometer with 150 MHz free spectral range and a finesse of 125 (Burleigh CFT 500). Absolute wavelength measurements were performed with a Burleigh WA 20 wavemeter with a precision of about $2 \times 10^{-2} \text{ cm}^{-1}$. The major systematic error in the experiment originated from thermal drift of the interferometer fringes which were simultaneously recorded with the spectrum. By measuring the same lines of the spectrum at different times the stability of the interferometer was found to be about 10 MHz/h. When this error is accounted for, the final uncertainty in the line positions is about $\pm 10 \text{ MHz}$.

The first few wavenumbers (blue edge) of the ${}^{\text{q}}\text{qQ}$ branch of the 14_0^1 band of $\text{C}_6\text{H}_5\text{D}$ were recorded. The spectra were linearized to the interferometer fringes and the positions of the rotational lines determined with the help of suitable computer programs.

3. Computational method

3.1. Line positions

The Hamiltonian \hat{H} employed for the evaluation of the rotational energy is Watson's A -reduction in the III^r representation [12]. A first-order perturbation calculation yields the eigenvalues

$$E_{\text{rot}}(J, K_a, K_c) = \langle H \rangle = W_0 - d_J J^2 (J+1)^2 - d_{JK} J(J+1) \langle \hat{J}_z^2 \rangle - d_K \langle \hat{J}_z^4 \rangle - d_{WJ} W_0 J(J+1) - d_{WK} W_0 \langle \hat{J}_z^2 \rangle. \quad (1)$$

W_0 is the eigenvalue of the rigid-rotor Hamiltonian \hat{H}_0 and J the total-angular-momentum quantum number. \hat{J}_z is the operator of the projection of the angular momentum on the figure axis and $\langle \hat{J}_z^2 \rangle$ and $\langle \hat{J}_z^4 \rangle$ are the average values of \hat{J}_z^2 and \hat{J}_z^4 respectively; they were evaluated as explained by Gordy and Cook [13]. The relations between the various d coefficients in eq. (1) with the Δ_J , Δ_{JK} , Δ_K , δ_J and δ_K quartic centrifugal distortion coefficients reported (see table 2) are given by Watson [12]. The energy levels are labelled by the quantum numbers J , K_a and K_c in the usual manner. The approximate energy formula

(as rendered by perturbation calculation) was used to simplify the numerical calculations. The validity of this approximation for the relatively low J values studied was carefully checked.

The rovibronic transition frequencies are then given by

$$\Delta\nu = \nu_0 + E'_{\text{rot}}(J', K'_a, K'_c) - E''_{\text{rot}}(J'', K''_a, K''_c), \quad (2)$$

where ν_0 is the vibronic origin of the ${}^1B_{2u}(14^1)$ state. In eq. (2) the prime denotes the excited and the double prime the ground states.

According to the theory of the asymmetric rotor [13] the rotational energy levels must satisfy the condition that $K_a + K_c = J$ or $J + 1$, and the rotational selection rules which apply to the ${}^{\text{aq}}Q$ branch studied are $\Delta J = \Delta K_a = \Delta K_c = 0$. Due to the significant asymmetry splitting observed (vide infra), the three rotational quantum numbers, J, K_a and K_c were used to identify unequivocally each level.

The analysis of the spectrum commenced by calculating a preliminary set of A'_v, B'_v and C'_v constants for benzene- d_1 from the known structural parameters of benzene- h_6 in the same electronically excited state

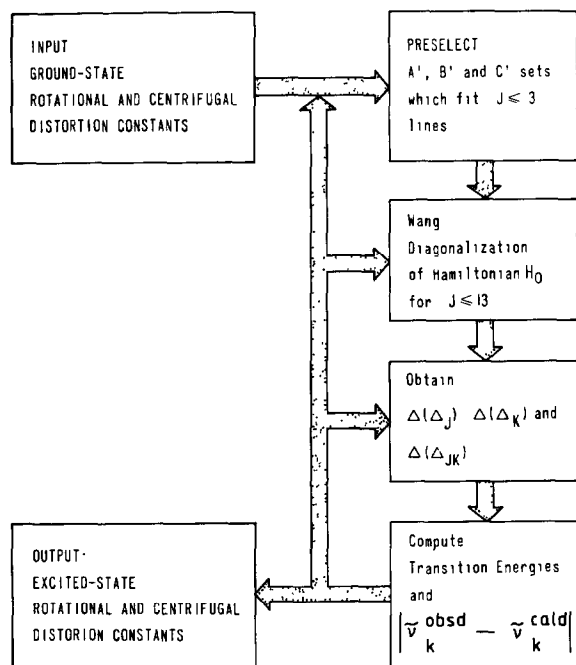


Fig. 1. Flow chart diagram showing the main segments and functioning of the algorithms used to evaluate the rotational constants from the measured spectrum.

[14]. By smoothly varying this preliminary set of constants and using the previously reported [11] ground-state constants, it was possible to reproduce the positions of the lines appearing in the first 3 GHz (blue edge) of the spectrum and therefore allow for the corresponding assignments. Following these initial assignments we determined an optimal set of rotational constants to reproduce these line positions. These constants in turn allowed for the assignments of even more lines, and repetition of this procedure finally rendered about 200 assigned lines. The final fit to the measured spectrum was done by a computational method whose overall functioning is sketched in a simplified flow-chart diagram in fig. 1 and explained briefly in the next paragraph.

The computational time required to fit the spectrum was drastically reduced by including a subroutine at the beginning of the algorithm which preselects, from a given range and increments, A'_v, B'_v and C'_v combinations which fit the strongest lines of the spectrum with $J \leq 3$ which have been assigned as mentioned above (second box in the flow-chart diagram in fig. 1). The fitting of this small portion of the spectrum was done by substituting $E'_{\text{rot}}(J', K'_a, K'_c)$ and $E''_{\text{rot}}(J'', K''_a, K''_c)$ in eq. (2) by the exact algebraic equations for the energy of an asymmetric rigid rotor given by Gordy and Cook [13] which are functions of A, B and C of both states involved in the transition; the assumption made here is that centrifugal distortion effects could be neglected for the low J values considered here. This resulting set of equations was solved by an iterative procedure in which the rotational constants of the excited state were each varied in increments of $2.5 \times 10^{-6} \text{ cm}^{-1}$ until the set of equations were all simultaneously satisfied within the experimental resolution. The complete Wang diagonalization of the rigid Hamiltonian H_0 , which is the next step in the algorithm, was then carried out only for the rotational constants thus preselected. For each set of A'_v, B'_v and C'_v investigated, the $\Delta(\Delta_J)$ centrifugal distortion constant difference was determined from the position of $K_c = 0$ lines; $\Delta(\Delta_K)$ and $\Delta(\Delta_{JK})$ were numerically evaluated.

$\Delta(\delta_J)$ and $\Delta(\delta_K)$ were constrained to zero. These constraints were used to limit the computational time needed to fit the spectrum. They were chosen because preliminary estimates yielded very small values for $\Delta(\delta_J)$ and $\Delta(\delta_K)$. The fact that the residuals

of all lines are nearly within the experimental uncertainty is taken as justification of the constraint. Oldani and Bauder [11], on the other hand, measured the ground-state positions of lines with J values as high as 39, and at an accuracy of 50 kHz, and were able to determine δ_J'' to be $6.4 \times 10^{-10} \text{ cm}^{-1}$ by constraining Δ_J'' and δ_K'' to zero in the fitting procedure. The best set of rotational and centrifugal distortion constants was the one which minimized the sum of the residuals

$$\sum_i |\nu_i(\text{obs.}) - \nu_i(\text{calc.})|, \quad (3)$$

where ν_i labels lines which are believed to be unperturbed and therefore selected for the fitting of the whole spectrum. The computational time required to complete each run increased strongly with the J value of the lines employed in the fitting. The largest J value of the selected lines used in eq. (3) did not exceed 13.

3.2. Line intensity

In order to simulate the experimental spectrum it was necessary to compute the intensity of each rovibronic transition. The relative strength of individual rovibronic lines was evaluated using

$$I = C g(J, K_a, K_c) A(J, K_a, K_c) \exp(-E_{\text{rot}}/K), \quad (4)$$

where C is a proportionality factor independent of the rotational transition, $A(J, K_a, K_c)$ is the rotational two-photon line strength factor expressed in terms of Wigner's $3-j$ symbols [1,15], $\exp(-E_{\text{rot}}/kT)$ is the Boltzmann factor, and $g(J, K_a, K_c)$ is the nuclear spin statistical weight. The number of nuclear spin states of benzene- d_1 ($\Pi_j(2I_j + 1)$), where I_j is the

Table 1
Statistical weights and symmetry species of the rotational levels of benzene- d_1 according to their K_a and K_c rotational quantum numbers

K_a	K_c	Γ_{rot}	Weight
e	e	A ₁	30
e	o	A ₂	30
o	e	B ₁	18
o	o	B ₂	18
total			96

nuclear spin of the j th nucleus) is 96. The individual distribution of the total nuclear spin statistical weight according to the K_a and K_c rotational quantum numbers was determined using the method reported by Job and Innes [16] and the results are shown in table 1.

Table 2
Spectroscopic constants (in cm^{-1} , Δ_0 and Δ_v in $\text{amu } \text{Å}^2$) of the ${}^1\text{B}_{2u}(14^1)$ excited and ${}^1\text{A}_{1g}$ ground vibrational states of benzene- d_1

${}^1\text{A}_{1g}(0_0)$ ground electronic state constants a)	
A_0	0.1897694(6)
B_0	0.1775873(6)
C_0	0.09171925(6)
$10^7 \Delta_J$	0.0
$10^7 \Delta_K$	-1.20(7)
$10^7 \Delta_{JK}$	-0.40(1)
$10^{10} \delta_J$	6.4
$10^{10} \delta_K$	0.0
κ	0.751513
Δ_0	0.038

${}^1\text{B}_{2u}(14^1)$ excited state presently determined constants b)

ν_0	39691.14(5)
A_v	0.1814350(25) c)
B_v	0.1699900(25) c)
C_v	0.0890550(25) c)
$10^7 \Delta(\Delta_J)$	4.48
$10^7 \Delta(\Delta_K)$	-5.8
$10^7 \Delta(\Delta_{JK})$	-14.85
$\Delta(\delta_J)$	0.0 d)
$\Delta(\delta_K)$	0.0 d)
κ	0.752219
Δ_v	-0.165

Derived centrifugal constants for the ${}^1\text{B}_{2u}(14^1)$ excited state b)

$10^7 DJ$	4.48
$10^7 DK$	-7.00(25)
$10^7 DJK$	-15.25(25)
$10^{10} \delta_J$	6.4
$10^{10} \delta_K$	0.0

a) The numbers in parentheses represent one standard deviation. Taken from ref. [11].

b) The numbers in parentheses are the increments employed in the fitting procedure (see text).

c) Calculated using the ground-state constants given in ref. [11].

d) Too small to be determined and therefore constrained to zero; see text.

e) Calculated with $\Delta_v = (1/C_v - 1/B_v - 1/A_v)$.

4. Results and discussion

The rotational and centrifugal constants which best fit the measured spectrum are listed in table 2. Included in the table are the ground electronic state rotational parameters reported by Oldani and Bauder [11] and the extrapolated origin of the vibronic transition studied.

The A'_v rotational constant of benzene- d_1 must be similar to the B'_v rotational constant of normal benzene. The comparison holds because the deuterium of the former species lies on the a axis. The A'_v value of $0.1814350 \text{ cm}^{-1}$ given in table 2 compares within $1.5 \times 10^{-4} \text{ cm}^{-1}$ with the B'_v value reported by Riedle et al. [5] for the same vibronic state in C_6H_6 . The inertial defect of the excited state calculated from the presently evaluated rotational constants is reported in table 2. $\Delta_v = -0.165 \text{ amu } \text{Å}^2$ for ben-

zene- d_1 compares with the value of $\Delta_v = -0.154 \text{ amu } \text{Å}^2$ of normal benzene calculated from the rotational constants of the same vibronic state [5]. The similarity of the inertial defects in benzene- d_1 and normal benzene is consistent with the small differences between their A'_v and B'_v rotational constants. This also suggests similar harmonic, anharmonic or Coriolis type contributions to the inertial defects in both molecules.

The most significant results of table 2 are the large values of $\Delta(\Delta_J)$, $\Delta(\Delta_K)$ and $\Delta(\Delta_{JK})$. Unfortunately the ground-state centrifugal constants previously evaluated [11] have been quoted as fitting parameters [17] which may have no physical meaning. Therefore the presently evaluated values of Δ'_J , Δ'_K and Δ'_{JK} for the excited state, derived here with the help of the ground-state constants, might not be accurate either. Other rotational branches (e.g. R or S)

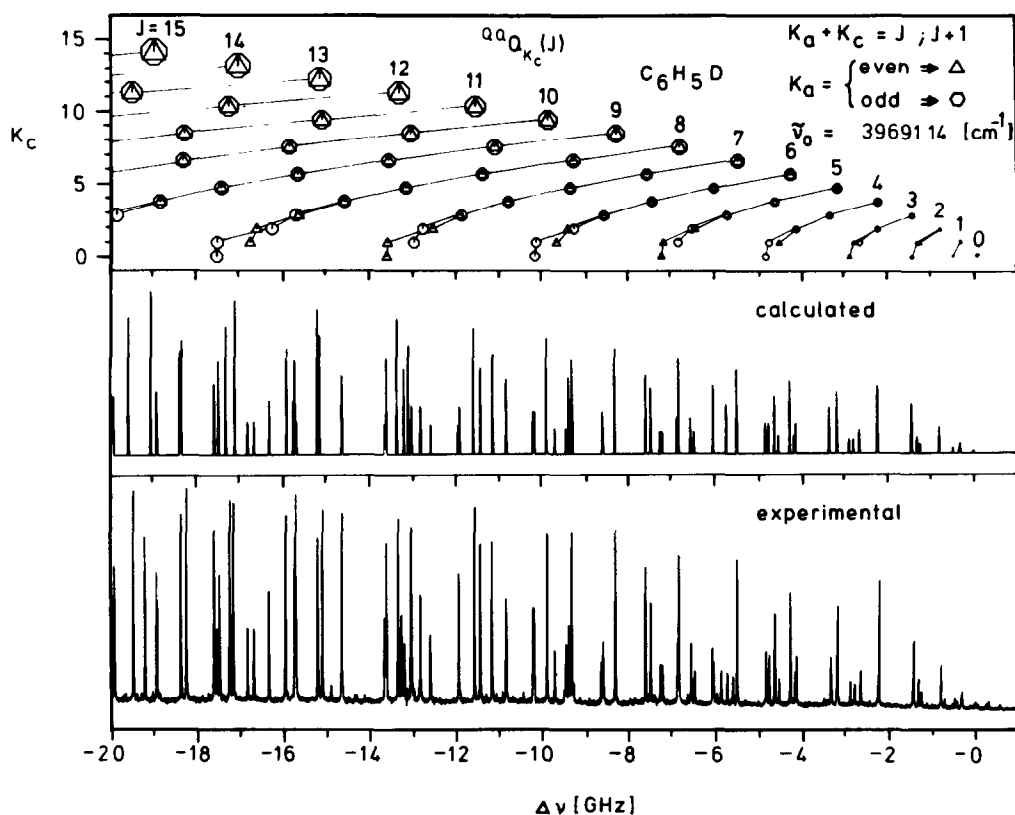


Fig. 2. Blue edge of the sub-Doppler two-photon spectrum of the 99Q branch of the 14_0^1 vibrational band of the ${}^1\text{B}_{2u} \leftarrow {}^1\text{A}_{1g}$ electronic system of $\text{C}_6\text{H}_5\text{D}$. At the bottom, the measured spectrum is shown, in the middle part the calculated one, and in the top the Fortrat diagram; all plotted on the same energy scale. In the Fortrat diagram, lines with constant values of J and K_c quantum numbers are connected with solid lines.

of the same vibronic band will soon be recorded in this laboratory and from them we expect to determine a new and perhaps more accurate set of ground-state centrifugal distortion constants.

Fig. 2 shows the first 20 GHz of the blue edge of the measured (bottom part) and calculated (middle part) spectra. The lineshape in the calculated spectrum is Gaussian with a linewidth of 12 MHz (fwhm). The spectrum is complex but its organization is well understood with the help of the Fortrat diagram shown in the upper part of the same figure and plotted in the same energy scale. For each J and K_c quantum number there are two K_a values (see section 3) according to $K_a + K_c = J$ or $J + 1$. They are indicated in the figure with triangles and circles for K_a even and odd, respectively. The size of these symbols is proportional to the corresponding transition intensity. Lines with the same J and K_a values are connected by lines in the diagram.

The energy separation between each pair of lines differing only in their K_a quantum numbers (K doublets) is proportional to the degree of asymmetry of the molecule and this is usually referred to as asymmetry splitting, δE . This splitting is expected to be largest for $K_c = 1$ and it increases quadratically with J (for constant K_c) according [13] to

$$\delta E \approx \frac{1}{2}(A - B)J(J + 1). \quad (5)$$

This is clearly seen in the Fortrat diagram. For instance, the splitting of lines with $K_a = 0$ and 1 for a given J value ($J = K_c$ lines) is not resolved in the spectrum. As K_c decreases, for the same J value, the asymmetry splitting becomes apparent in the spectrum and it reaches a maximum at $K_c = 1$ where the present resolution clearly resolves these pairs of lines for all J values assigned.

The lines with K_a odd of the ${}^{99}\text{Q}_5(J)$ subbranch show small and quite regular perturbations which are manifested in the form of a larger than expected asymmetry splitting. The splitting is not observed for the $J = 5$ doublet. The calculations predict a separation between the K_a components of $K_c = 5$ lines with $J \geq 5$ smaller than 1 MHz but the measured lines are separated by 60 ± 5 MHz in most cases. This is indicated in table 3 and clearly seen in fig. 3. The intensity of the perturbed lines is well reproduced by eq. (4), and because each anomalous ${}^{99}\text{Q}_5$ K doublet shows a 10 : 6 ratio according to their spin statistical

Table 3
Observed and calculated asymmetry splitting for $K_c = 5$ lines

J	Obs. (MHz)	Calc. (MHz)
5	0	<1
6	45	<1
7	65	<1
8	67	<1
9	60	<1
10	56	<1
11	57	<1
12	56	<1
13	62	<1

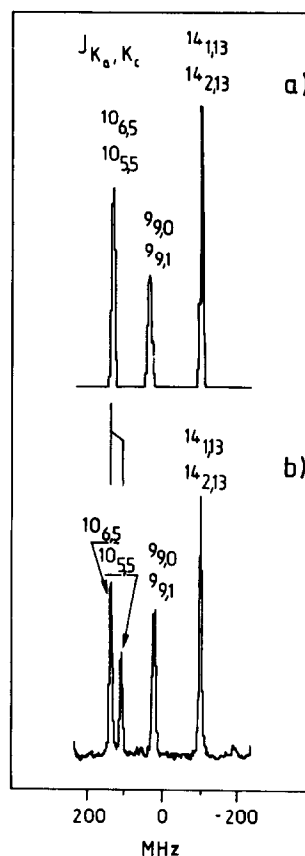


Fig. 3. Calculated (a) and measured (b) parts of the ${}^{99}\text{Q}$ branch of the 14_0^1 two-photon Doppler-free band of $\text{C}_6\text{H}_5\text{D}$. In the measured spectrum, instead of one unresolved line corresponding to the $10_{6,5}$ and $10_{5,5}$ transitions, there are two well separated lines. The assignment of these lines was made by taking into account their 10 : 6 intensity ratio according to the nuclear spin statistical weights (see text).

weights, their corresponding assignments are readily made.

Fung and Ramsay [18] have observed an anomalous asymmetry splitting of the 1R_3 branch of the 4_0^1 band of the $\tilde{A} \leftarrow \tilde{X}$ electronic system of thioformaldehyde. In this case the perturbations were found to be very irregular and in some cases as large as 300 MHz. The perturbations are magnetically insensitive, indicating that they are caused by high vibrational levels of the ground electronic state (the S_1-S_0 energy gap for H_2CS is only about 16400 cm^{-1} and therefore level density is rather small). This possibility seems quite improbable in the case of C_6H_5D . This was discussed in a previous work [8] for the case of C_6H_6 considering that at 40000 cm^{-1} , the S_1-S_0 energy gap in benzene, the density of vibrational states in S_0 is too high to produce the observed splitting of lines. The possibility of perturbations from the $T_1({}^3B_{1u})$ and $T_2({}^3E_{1u})$ electronic states has also been excluded [8,9] on the basis of recent lifetime measurements [19] and density of isoenergetic states. It has been concluded in more recent work [8] that the interactions in benzene- h_6 are due to perpendicular Coriolis coupling between different, nearly degenerate, vibrational states of S_1 . A preliminary analysis of the present results indicates that the observed perturbations in benzene- d_1 are consistent with a -type parallel Coriolis coupling with the selection rules $\Delta J = 0$, $\Delta K_a = 0$ and $\Delta K_c = -1$. By similar arguments as for benzene- h_6 [8,9], but considering that, because of the lower symmetry of the deuterated species the number of vibrational states to which the ${}^1B_{2u}(14^1)$ level of benzene- d_1 can couple are much greater than in benzene- h_6 , we conclude that the perturbing state is most likely another vibrational state of the S_1 manifold.

Perturbations in some other individual lines at transition energies more than $\approx 30\text{ GHz}$ from the origin have been observed but the fitting in this spectral region is not optimal and the density of lines at these energies is quite high making their identification difficult.

The observed and calculated positions of the lines appearing in the first 30 GHz (1 cm^{-1}) of the spectrum, together with their residuals, are listed in table 4. Lines used in the fitting procedure are indicated in the table. To obtain an even better fitting an exact diagonalization of the Watson Hamiltonian, instead

Table 4
Observed and calculated positions, assignments and residuals of all the lines appearing in the first 30 GHz part of the 1R_3 branch of the $S_1(14^1) \leftarrow S_0$ transition in benzene- d_1

J	K_a	K_c	Obs. (GHz)	Calc. (GHz)	Residuals (MHz)
1	0	1	-0.308	-0.308	-1
1	1	1	-0.328	-0.330	1
1	1	0	-0.475	-0.478	3
2	0	2	-0.796	-0.794	-2 a)
2	1	2	-0.796	-0.796	0 a)
2	1	1	-1.242	-1.241	-1 a)
2	2	1	-1.290	-1.307	18 a)
2	2	0	-1.431	-1.436	5 a)
3	0	3	-1.431	-1.429	-1 a)
3	1	3	-1.431	-1.430	-1 a)
3	1	2	-2.210	-2.218	8 a)
3	2	2	-2.232	-2.229	-3 a)
3	2	1	-2.635	-2.643	8 a)
3	3	1	-2.769	-2.776	7 a)
3	3	0	-2.878	-2.879	1 a)
4	0	4	-2.210	-2.218	8 a)
4	1	4	-2.210	-2.218	8 a)
4	1	3	-3.318	-3.335	18 a)
4	2	3	-3.318	-3.336	19 a)
4	2	2	-4.105	-4.111	7 a)
4	3	2	-4.137	-4.144	7 a)
4	3	1	-4.510	-4.518	8 a)
4	4	1	-4.738	-4.738	0 a)
4	4	0	-4.811	-4.814	4 a)
5	0	5	-3.162	-3.157	-5 a)
5	1	5	-3.162	-3.157	-5 a)
5	1	4	-4.609	-4.601	-8
5	2	4	-4.609	-4.601	-8
5	3	3	-5.701	-5.721	19
5	3	2	-6.458	-6.470	11
5	4	2	-6.542	-6.542	0
5	4	1	-6.860	-6.868	8
5	5	1	-7.202	-7.196	-6
5	5	0	-7.250	-7.249	-2
6	0	6	-4.251	-4.240	-11 a)
6	1	6	-4.251	-4.240	-11 a)
6	1	5	-6.025	-6.015	-10
6	2	5	-6.049	-6.015	-34
6	2	4	-7.477	-7.462	-15
6	3	4	-7.477	-7.462	-15
6	3	3	-8.616	-8.573	-43
6	4	3	-8.568	-8.584	16
6	4	2	-9.260	-9.294	33
6	5	2	-9.432	-9.427	-5
6	5	1	-9.693	-9.701	8
6	6	1	-10.166	-10.153	-13
6	6	0	-10.196	-10.188	-9
7	0	7	-5.476	-5.461	-16 a)
7	1	7	-5.476	-5.461	-16 a)
7	1	6	-7.594	-7.573	-22

Table I continued

<i>J</i>	<i>K_a</i>	<i>K_c</i>	Obs. (GHz)	Calc. (GHz)	Residuals (MHz)	<i>J</i>	<i>K_a</i>	<i>K_c</i>	Obs. (GHz)	Calc. (GHz)	Residuals (MHz)
7	2	6	-7.594	-7.573	-22	10	3	7	-18.363	-18.332	-31
7	2	5	-9.300	-9.353	53	10	4	7	-18.363	-18.332	-31
7	3	5	-9.365	-9.353	-12	10	4	6	-20.480	-20.468	-12
7	3	4	-10.820	-10.802	-18	10	5	6	-20.480	-20.468	-12
7	4	4	-10.820	-10.803	-17	10	5	5	-22.222	-22.264	41
7	4	3	-11.914	-11.901	-12	10	6	5	-22.279	-22.265	-15
7	5	3	-11.914	-11.930	16	10	6	4	-23.661	-23.703	42
7	5	2	-12.574	-12.585	11	10	7	4	-23.692	-23.723	31
7	6	2	-12.805	-12.804	-2	10	7	3	-24.674	-24.709	36
7	6	1	-12.961	-13.023	62	10	8	3	-24.796	-24.889	94
7	7	1	-13.641	-13.614	-28	10	8	2	-25.235	-25.329	94
7	7	0	-13.641	-13.635	-7	10	9	2	-25.896	-25.926	30
8	0	8	-6.827	-6.812	-15 a)	10	9	1	-25.965	-26.010	44
8	1	8	-6.827	-6.812	-15 a)	10	10	1	-27.005	-27.044	39
8	1	7	-9.300	-9.267	-32	10	10	0	-27.005	-27.048	43
8	2	7	-9.300	-9.267	-32	11	0	11	-11.551	-11.556	4 a)
8	2	6	-11.416	-11.387	-29	11	1	11	-11.551	-11.556	4 a)
8	3	6	-11.416	-11.387	-29	11	1	10	-15.084	-15.089	5 a)
8	3	5	-13.178	-13.173	-5	11	2	10	-15.084	-15.089	5 a)
8	4	5	-13.245	-13.173	-72	11	2	9	-18.236	-18.271	35 a)
8	4	4	-14.635	-14.622	-13	11	3	9	-18.236	-18.271	35 a)
8	5	4	-14.635	-14.625	-10	11	3	8	-21.127	-21.106	-22
8	5	3	-15.691	-15.701	10	11	4	8	-21.127	-21.106	-22
8	6	3	-15.711	-15.760	49	11	4	7	-23.602	-23.595	-7
8	6	2	-16.321	-16.351	30	11	5	7	-23.602	-23.595	-7
8	7	2	-16.668	-16.676	8	11	5	6	-25.729	-25.740	11
8	7	1	-16.818	-16.843	25	11	6	6	-25.729	-25.741	12
8	8	1	-17.589	-17.580	-10	11	6	5	-27.449	-27.539	90
8	8	0	-17.589	-17.593	3	11	7	5	-27.506	-27.542	36
9	0	9	-8.293	-8.286	-8 a)	11	7	4	-	-28.964	b)
9	1	9	-8.293	-8.286	-8 a)	11	8	4	-28.917	-29.005	88
9	1	8	-11.144	-11.091	-53	11	8	3	-	-29.923	b)
9	2	8	-11.144	-11.091	-53	12	0	12	-13.325	-13.329	4
9	2	7	-13.595	-13.557	-38	12	1	12	-13.325	-13.329	4
9	3	7	-13.595	-13.557	-38	12	1	12	-17.230	-17.241	11
9	3	6	-15.711	-15.685	-26	12	2	11	-17.230	-17.241	11
9	4	6	-15.711	-15.685	-26	12	2	10	-20.772	-20.796	23
9	4	5	-17.462	-17.476	14	12	3	10	-20.772	-20.796	23
9	5	5	-17.522	-17.476	-46	12	3	9	-23.911	-23.997	85
9	5	4	-18.924	-18.922	-3	12	4	9	-23.911	-23.997	85
9	6	4	-18.924	-18.931	7	12	5	7	-29.315	-29.349	35
9	6	3	-19.906	-19.970	64	12	6	7	-29.315	-29.349	35
9	7	3	-20.022	-20.078	56	13	0	13	-15.192	-15.177	-15
9	7	2	-20.539	-20.596	57	13	1	13	-15.192	-15.177	-15
9	8	2	-21.024	-21.048	24	13	1	12	-19.465	-19.479	14
9	8	1	-21.197	-21.169	-27	13	2	12	-19.465	-19.479	14
9	9	1	-22.044	-22.056	11	13	2	11	-	-23.417	b)
9	9	0	-22.044	-22.063	19	13	3	11	-	-23.417	b)
10	0	10	-9.872	-9.870	-2 a)	13	3	10	-27.039	-26.994	-44
10	1	10	-9.872	-9.870	-2 a)	13	4	10	-27.039	-26.994	-44
10	1	9	-13.011	-13.035	25	14	0	14	-17.146	-17.085	-61
10	2	9	-13.031	-13.035	5	14	1	14	-17.146	-17.085	-61
10	2	8	-15.935	-15.855	-80	14	1	13	-21.791	-21.790	-1
10	3	8	-15.935	-15.855	-80	14	2	13	-21.791	-21.790	-1

Table 1 continued

<i>J</i>	<i>K_a</i>	<i>K_c</i>	Obs. (GHz)	Calc. (GHz)	Residual (MHz)
14	2	12	-26.078	-26.122	45
14	3	12	-26.078	-26.122	45
15	0	15	-	-19.037	b)
15	1	15	-	-19.037	b)
15	1	14	-24.205	-24.158	-48
15	2	14	-24.205	-24.158	-48
16	0	16	-21.024	-21.017	-7
16	1	16	-21.024	-21.017	-7
16	1	15	-	-26.567	b)
16	2	15	-	-26.567	b)
17	0	17	-	-23.005	b)
17	1	17	-	-23.005	b)
19	0	19	-26.930	-26.931	1
19	1	19	-26.930	-26.931	1
20	0	20	-28.862	-28.826	-35
20	1	20	-28.862	-28.826	-35

a) Lines used in the fitting procedure.

b) This line has not been assigned and most likely it is perturbed.

of the perturbation approximation used now, is needed and the constraints on the δ_J and δ_K constants should be lifted. In addition many more lines need to be included in the fit and this would imply lines with quite high quantum numbers which could only be fitted provided sextic centrifugal distortion constants are included in the Hamiltonian.

5. Conclusions

The most significant result from the present analysis is the important role of the centrifugal distortion effects in the rotationally resolved spectra of large molecules. Because these effects become apparent for lines with *J* values larger than about 10, they are not likely to be detected in the spectra of rotationally cold molecules. For this reason, for molecules with a reasonable density of rotational lines, room-temperature Doppler-free two-photon absorption appears more advantageous than jet techniques for recording rotationally resolved spectra. It is apparent from the present results that the rotational constants reported by Thakur and Goodman [20] for several benzene derivatives, as calculated from band contour analysis using Gora's formula [21], are probably inaccurate.

Acknowledgement

The authors gratefully acknowledge valuable experimental help by H. Stepp in the recording of the spectrum. They want to thank Professor E.W. Schlag for his stimulating interest in this work and one of them (AEB) wishes to thank him for his hospitality during his stay at this Institute.

References

- [1] S.H. Lin, Y. Fujimura, H.J. Neusser and E.W. Schlag, Multiphoton spectroscopy of molecules (Academic Press, New York, 1984), and references therein.
- [2] L. Goodman and R.P. Rava, *Advan. Laser Spectry.* 1 (1982) 21.
- [3] A. Sur, J. Knee and P. Johnson, *J. Chem. Phys.* 77 (1982) 654.
- [4] L. Wunsch, H.J. Neusser and E.W. Schlag, *Chem. Phys. Letters* 31 (1975) 433.
- [5] E. Riedle, H.J. Neusser and E.W. Schlag, *J. Chem. Phys.* 75 (1981) 4231.
- [6] E. Riedle, H.J. Neusser and E.W. Schlag, *J. Phys. Chem.* 86 (1982) 4847.
- [7] E. Riedle and H.J. Neusser, *J. Chem. Phys.* 80 (1984) 4686.
- [8] E. Riedle, H. Stepp and H.J. Neusser, *Chem. Phys. Letters* 110 (1984) 452.
- [9] E. Riedle and H.J. Neusser, in preparation.
- [10] R. Rava, L. Goodman and K. Krogh-Jespersen, *Chem. Phys. Letters* 68 (1979) 337; L. Goodman and R.P. Rava, in: *Advances in chemical physics*, eds. I. Prigogine and S.A. Rice (Wiley, New York, 1983).
- [11] M. Oldani and A. Bauder, *Chem. Phys. Letters* 108 (1984) 7.
- [12] J.K.C. Watson, *J. Chem. Phys.* 46 (1966) 1935.
- [13] W. Gordy and R.L. Cook, *Techniques of chemistry*, Vol. 18, 3rd. Ed. *Microwave molecular spectra* (Wiley, New York, 1984).
- [14] J.H. Callomon, T.M. Dunn and I.M. Mills, *Phil. Trans. Roy. Soc. (London)* 259A (1966) 499.
- [15] F. Metz, W.E. Howard, L. Wunsch, H.J. Neusser and E.W. Schlag, *Proc. Roy. Soc. A* 363 (1978) 381; W.M. McClain and R.A. Harris, in: *Excited states*, Vol. 3, ed. E.C. Lim (Academic Press, New York, 1977) p. 1.
- [16] V.A. Job and K.K. Innes, *J. Mol. Spectry.* 71 (1978) 299.
- [17] M. Oldani, private communication.
- [18] K.H. Fung and D.A. Ramsay, *J. Phys. Chem.* 88 (1984) 395.
- [19] U. Schubert, E. Riedle and H.J. Neusser, *J. Chem. Phys.*, to be published.
- [20] S.N. Thakur and L. Goodman, *J. Chem. Phys.* 78 (1982) 4356.
- [21] K. Gora, *J. Mol. Spectry.* 16 (1965) 378.